Simultaneous Localization and Channel Estimation for 5G mmWave MIMO Communications

Bingpeng Zhou[†], Risto Wichman[‡], Lei Zhang[*], and Zhiyong Luo[†]
[†]School of Electronics and Communication Engineering, Sun Yat-sen University, Shenzhen 518000, China
[‡]Department of Signal Processing and Acoustics, Aalto University, Espoo 02150, Finland
[*]Jame Watt School of Engineering, University of Glasgow, Glasgow, G12 8QQ, UK
zhoubp3@mail.sysu.edu.cn, risto.wichman@aalto.fi, lei.zhang@glasgow.ac.uk, luozhy57@mail.sysu.edu.cn

***Abstract*—In this paper, we are interested in the joint estimate of user equipment (UE) location and orientation for millimeter-wave multi-input-multi-output (mmWave MIMO) systems. In practice, mmWave signals suffer from small-scale fading, which degrades UE localization. Moreover, mmWave MIMO-based UE localization is a non-convex optimization problem, and the brute-force application of conventional optimization methods will result in a poor solution or lead to large computational cost. In order to address the above challenges, we propose a novel simultaneous localization and channel estimate (SLCE) algorithm, where the UE location parameters and small-scale fading coefficients are jointly optimized. In such a case, the disturbance of small-scale fading on UE localization is alleviated. Thanks to our problem-specific update rule design, the proposed SLCE algorithm achieves a large performance gain over existing baseline methods.**

***Index Terms*—Localization, 5G mmWave MIMO communications, channel estimate, small-scale channel fading.**

I. Introduction

MILLIMETER-wave (mmWave) and massive multiple-input-multiple-output (MIMO) are promising candidate enabling technologies for 5G communication systems [1], [2]. A multitude of earlier research works have been conducted to demonstrate the great benefit of mmWave MIMO for efficient data transmission [3], [4]. Nevertheless, its potential for wireless localization is not fully studied, in spite of up-to-date advances [5]. User equipment (UE) location knowledge is indispensable for location-aware 5G communication networks [6]– [8]. Hence, investigation of UE localization using mmWave MIMO is demanded.

It is shown in [5] that UE location parameters (i.e., position and orientation) can be gained via leveraging time-of-flight and angular gain of mmWave MIMO signals. However, it is challenging to exploit mmWave MIMO-based UE localization due to the following reasons.

- *Small-Scale Fading*: In practice, mmWave signals suffer from fast small-scale fading, where small-scale fading coefficients are unknown and vary dramatically. This extends the uncertainty set of UE localization problem and thus degrades the UE localization performance.
- *Non-Convexity Nature*: UE localization is a non-convex optimization problem due to nonlinear signal propagation models. Conventional brute-force solutions may result in poor solutions or lead to high computational cost [9].

UE localization and channel estimate for conventional radio networks have been devised in past decades, e.g., wideband localization [10], WiFi localization and wireless sensor network localization [11]– [14]. However, the direct application of such conventional localization algorithms to mmWave MIMO systems will inevitably lead to a bad performance, due to the different propagation nature of mmWave MIMO signals. Hence, a dedicated development of mmWave MIMO-based localization algorithm is needed. Upon now, there are a few works on mmWave MIMO-based UE localization. In [5], UE localization using mmWave signals is studied, and a three-stage optimization method integrating orthogonal matching pursuit, expectation maximization and Gauss-Seidel iteration methods is developed. However, this algorithm is computational complex. Hence, a light-weight UE localization solution for mmWave MIMO systems is desired.

In this paper, we are concerned with the mmWave MIMO-based UE localization under small-scale channel fading. To address above technical challenges, we propose a novel simultaneous localization and channel estimate (SLCE) algorithm, where the UE location parameters and small-scale fading coefficients are jointly estimated. In such a case, the disturbance of small-scale fading on UE localization is alleviated. Thanks to the problem-specific update rule design, the proposed SLCE algorithm will achieve a huge performance gain over existing state-of-the-art baseline methods.

The remainder of this paper is organized as follows. Section II presents system model. The proposed SLCE algorithm is presented in Section III. Simulations results are presented in Section IV. Finally, Section V concludes the paper.

II. System Model

In this section, we elaborate the system setup and signal model for mmWave-based UE localization.

A. System Setup

We consider a mmWave OFDM system with J base stations (BS), one UE and N'_{C} subcarriers, as shown in Fig. 1. Each BS

This work was supported by National Natural Science Foundation of China under Grant 62001526, and in part by the Natural Science Foundation of Guangdong Province under Grant 2021A1515012021.

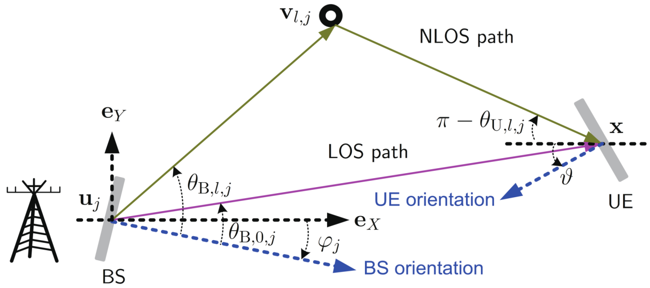

Fig. 1. Illustration of the mmWave MIMO system for SLCE.

has N_{B} antennas whereas the UE has N_{U} antennas. BSs will transmit training pilots for estimating UE location parameters. We assume OFDM signaling and the length of the cyclic prefix is assumed to exceed the maximum delay.

We focus on one interval of channel coherence time within which the large-scale multipath parameters, e.g., time-of-arrival (TOA), angle-of-departure (AOD) and angle-of-arrival (AOA) of each path are constant. We assume the small-scale fading coefficients to be constant within one time slot. The first M symbols are (known) pilots. Let $\boldsymbol{\omega}_j[n,m] \in \mathbb{C}^{N_{\mathrm{B}}}$ be the mth training symbols transmitted from the N_{B} antennas of the jth BS on the nth subcarrier [15].

In addition, we assume that signals from different BSs can be identified by the UE via certain frequency-division-based coordinated multiple point transmission methods [16]. The N'_{C} subcarriers of each pilot are fairly allocated to those J BSs via predefined scheduling procedures, and thus each BS has $N_{\mathrm{C}} = N'_{\mathrm{C}}/J$ subcarriers to transmit training pilots (we assume N_{C} is an integer). For instance, the subcarriers of the jth BS are given by $\{j, j+J, \cdots, j+(N_{\mathrm{C}}-1)J\}$. We use $\Theta_j = \{j, j+J, \cdots, j+(N_{\mathrm{C}}-1)J\}$ to denote the index set of subcarriers associated with the jth BS. Let $\boldsymbol{\omega} \in \mathbb{C}^{N_{\mathrm{B}}JN_{\mathrm{C}}M} = \mathrm{vec}[\boldsymbol{\omega}_j[n,m] | \forall n = 1 \in \Theta_j, \forall m = 1\!:\!M, \forall j = 1\!:\!J]$, and N'_{C} is the number of subcarriers.

B. Channel Model

We consider limited scattering in mmWave MIMO channel. Specifically, let $\mathbf{u}_j \in \mathbb{R}^2$ and $\varphi_j \in [-\pi, \pi)$ be the known coordinate and angular position of the jth BS. Let $\mathbf{x} \in \mathbb{R}^2$ and $\vartheta \in [-\pi, \pi)$ be the unknown position and orientation, respectively, of the UE. There are $L+1$ paths in the scattering channel from each BS where the first path corresponds to line-of-sight (LOS) channel and the other paths are non-line-of-sight (NLOS) channels. Let $\tau_{l,j}$, $\theta_{\mathrm{B},l,j}$ and $\theta_{\mathrm{U},l,j}$ denote the TOA, AOD and AOA of the lth path associated with the jth BS, respectively, which are unknown scalars. For each NLOS path, there is a scatterer with unknown location, as shown in Fig. 1. Let $\mathbf{v}_{l,j} \in \mathbb{R}^2$ be unknown scatter location associated with the lth path of the jth BS. In addition, as per the mmWave signal propagation characteristics [5], we consider the single-bounce reflection for NLOS paths.

Given multipath parameters $\tau_{l,j}$, $\theta_{\mathrm{B},l,j}$ and $\theta_{\mathrm{U},l,j}$, $\forall l$, the channel matrix $\widetilde{\mathbf{H}}_j[n] \in \mathbb{C}^{N_{\mathrm{B}} \times N_{\mathrm{U}}}$ between the jth BS and the user on the nth subcarrier is cast as [5]

$$\widetilde{\mathbf{H}}_j[n] = \mathbf{V}_{\mathrm{U},j}[n]\mathbf{A}_{\mathrm{U},j}[n]\mathbf{H}_j[n]\mathbf{A}^{\mathrm{H}}_{\mathrm{B},j}[n],$$

where $\mathbf{A}_{\mathrm{B},j}[n] \in \mathbb{C}^{N_{\mathrm{B}} \times (L+1)}$ is the steering matrix of the jth BS antenna array on the nth subcarrier, and $\mathbf{A}_{\mathrm{U},j}[n] \in \mathbb{C}^{N_{\mathrm{U}} \times (L+1)}$ is the response matrix of UE antenna array on the nth subcarrier, which depend on the unknown angular parameters such as $\theta_{\mathrm{B},l,j}$ and $\theta_{\mathrm{U},l,j}$, given by

$$\mathbf{A}_{\mathrm{B},j}[n] = N_{\mathrm{B}}^{-\frac{1}{2}}[\mathbf{a}_{\mathrm{B},n}(\theta_{\mathrm{B},0,j}), \cdots, \mathbf{a}_{\mathrm{B},n}(\theta_{\mathrm{B},L,j})], \quad (1)$$

$$\mathbf{a}_{\mathrm{B},n}(\theta_{\mathrm{B},l,j}) = \mathrm{vec}[e^{-\mathrm{j}\frac{d_{\mathrm{B}}\pi}{\lambda_n}(t-1)\sin\theta_{\mathrm{B},l,j}} | \forall t = 1:N_{\mathrm{B}}], \quad (2)$$

$$\mathbf{A}_{\mathrm{U},j}[n] = N_{\mathrm{U}}^{-\frac{1}{2}}[\mathbf{a}_{\mathrm{U},n}(\theta_{\mathrm{U},0,j}), \cdots, \mathbf{a}_{\mathrm{U},n}(\theta_{\mathrm{U},L,j})], \quad (3)$$

$$\mathbf{a}_{\mathrm{U},n}(\theta_{\mathrm{U},l,j}) = \mathrm{vec}[e^{-\mathrm{j}\frac{d_{\mathrm{A}}\pi}{\lambda_n}(r-1)\sin\theta_{\mathrm{U},l,j}} | \forall r = 1:N_{\mathrm{U}}], \quad (4)$$

in which $\mathrm{j} = \sqrt{-1}$, λ_n is the wavelength associated with subcarrier n, and d_{A} is the distance between antenna elements.

In addition, $\mathbf{H}_j[n] \in \mathbb{C}^{(L+1)\times(L+1)}$ is the frequency-domain channel matrix on the nth subcarrier:

$$\mathbf{H}_j[n] = \sqrt{N_{\mathrm{B}}N_{\mathrm{U}}}\,\mathrm{diag}\{h_{l,j}e^{-\mathrm{j}2\pi\frac{n}{N'_{\mathrm{C}}T_s}\tau_{l,j}} | \forall l = 0:L\}, \quad (5)$$

where $h_{l,j}$ is the unknown small-scale fading coefficient of the lth path (path loss is absorbed into the small-scale fading coefficient), and T_s is the sampling period. Let $\mathbf{h} \in \mathbb{C}^{J(L+1)} = \mathrm{vec}[h_{l,j} | \forall l = 0\!:\!L, \forall j = 1\!:\!J]$. We assume that $\mathbf{h}$ follows an independent and identical complex Gaussian distribution, i.e., $\mathbf{h} \sim \mathcal{N}_{\mathbb{C}}(\mathbf{h}|\mathbf{0}, \boldsymbol{\Sigma})$ with covariance matrix $\boldsymbol{\Sigma}$.[1]

The relationship between location parameters $\{\mathbf{x}, \mathbf{v}_{l,j}, \vartheta\}$ and propagation parameters $\{\tau_{l,j}, \theta_{\mathrm{B},l,j}, \theta_{\mathrm{U},l,j}\}$ is given by

$$\tau_{0,j} = \frac{\|\mathbf{x}-\mathbf{u}_j\|_2}{c}, \quad (6)$$

$$\tau_{l,j} = \frac{\|\mathbf{x}-\mathbf{v}_{l,j}\|_2 + \|\mathbf{u}_j-\mathbf{v}_{l,j}\|_2}{c}, \; l>0, \quad (7)$$

$$\theta_{\mathrm{B},0,j} = \arccos\left(\frac{(\mathbf{x}-\mathbf{u}_j)^\top\mathbf{e}_X}{\|\mathbf{x}-\mathbf{u}_j\|_2}\right) - \varphi_j, \quad (8)$$

$$\theta_{\mathrm{B},l,j} = \arccos\left(\frac{(\mathbf{v}_{l,j}-\mathbf{u}_j)^\top\mathbf{e}_X}{\|\mathbf{v}_{l,j}-\mathbf{u}_j\|_2}\right) - \varphi_j, \; l>0 \quad (9)$$

$$\theta_{\mathrm{U},0,j} = \pi + \arccos\left(\frac{(\mathbf{x}-\mathbf{u}_j)^\top\mathbf{e}_X}{\|\mathbf{x}-\mathbf{u}_j\|_2}\right) - \vartheta, \quad (10)$$

$$\theta_{\mathrm{U},l,j} = \pi + \arccos\left(\frac{(\mathbf{x}-\mathbf{v}_{l,j})^\top\mathbf{e}_X}{\|\mathbf{x}-\mathbf{v}_{l,j}\|_2}\right) - \vartheta, \; l>0, \quad (11)$$

where c is the light speed, and $\mathbf{e}_X = [1,0]^\top$. For ease of notation, let $\boldsymbol{\alpha} \in \mathbb{R}^3 = [\mathbf{x}; \vartheta]$ be the unknown UE location parameters, let $\mathbf{v} \in \mathbb{R}^{2JL} = \mathrm{vec}[\mathbf{v}_{l,j} | \forall l = 1\!:\!L, \forall j = 1\!:\!J]$, and let $\boldsymbol{\beta} \in \mathbb{C}^{2JL+3} = [\boldsymbol{\alpha}; \mathbf{v}]$.

C. Received Measurement Signal

Let $\mathbf{z}_j[n,m] \in \mathbb{C}^{N_{\mathrm{U}}}$ be the observation signal, i.e., the mth received pilot signal vector on subcarrier n from the jth BS at the kth time slot, in which we have omitted the index of time

[1]Generally, LOS and NLOS channels have different statistics. Here we assume identical statistics to consider a challenging environment.

slot when there is no ambiguity. Furthermore, the observation signal $\mathbf{z}_j[n,m]$ is given by [5]

$$\mathbf{z}_j[n,m] = \widetilde{\mathbf{H}}_j[n]\,\boldsymbol{\omega}_j[n,m] + \boldsymbol{\epsilon}_j[n,m], \tag{12}$$

where $\boldsymbol{\epsilon}_j[n,m] \in \mathbb{C}^{N_{\mathrm{U}}}$ is the noise vector at the UE.

Let $\mathbf{z} \in \mathbb{C}^{N_{\mathrm{U}}N_{\mathrm{C}}MJ} = \mathrm{vec}[\mathbf{z}_j[n,m]|\forall n \in \Theta_j, \forall m = 1:M, \forall j = 1:J]$ and $\boldsymbol{\epsilon} \in \mathbb{C}^{N_{\mathrm{U}}N_{\mathrm{C}}MJ} = \mathrm{vec}[\boldsymbol{\epsilon}_j[n,m]|\forall n \in \Theta_j, \forall j = 1:J, \forall m = 1:M]$. Given a training symbol $\boldsymbol{\omega}$, the measurement signal $\mathbf{z}$ can be expressed as a function of the slow-timescale location parameter $\boldsymbol{\beta}$, the fast-timescale channel vector $\mathbf{h}$ and the noise vector $\boldsymbol{\epsilon}$ as

$$\mathbf{z} = \mathbf{g}(\boldsymbol{\beta}, \mathbf{h}) + \boldsymbol{\epsilon}, \tag{13}$$

where we assume that $\boldsymbol{\epsilon}$ follows a zero-mean complex Gaussian distribution, i.e., $\boldsymbol{\epsilon} \sim \mathcal{N}_{\mathbb{C}}(\boldsymbol{\epsilon}|\mathbf{0}, \sigma^2\mathbf{I})$ with variance σ^2. In addition, $\mathbf{g}(\boldsymbol{\beta}, \mathbf{h})$ is the measurement function, given by

$$\mathbf{g}(\boldsymbol{\beta}, \mathbf{h}) = \mathbf{G}(\boldsymbol{\beta})\mathbf{h}, \tag{14}$$

in which $\mathbf{G}(\boldsymbol{\beta}) \in \mathbb{C}^{N_{\mathrm{U}}N_{\mathrm{C}}MJ \times J(L+1)}$ is the coefficient matrix of channel vector $\mathbf{h}$, which is dependent on the unknown location parameter $\boldsymbol{\beta}$ and given by [5]

$$\mathbf{G}(\boldsymbol{\beta}) = \mathrm{diag}[\mathbf{G}_j|\forall j = 1:J], \tag{15}$$

$$\mathbf{G}_j \in \mathbb{C}^{N_{\mathrm{U}}N_{\mathrm{C}}M \times (L+1)} = \mathrm{vec}[\mathbf{g}_j^{(r)\mathrm{H}}[n,m]|\forall r, \forall n, \forall m], \tag{16}$$

$$\mathbf{g}_j^{(r)}[n,m] \in \mathbb{C}^{L+1} = \mathrm{vec}[\mathrm{g}_{l,j}^{(r)}[n,m]|\forall l = 0:L], \tag{17}$$

$$\mathrm{g}_{l,j}^{(r)}[n,m] = \boldsymbol{\omega}_j^{\mathrm{H}}[n,m]\boldsymbol{\mu}_{l,j,n}^{(r)}, \tag{18}$$

$$\boldsymbol{\mu}_{l,j,n}^{(r)} \in \mathbb{C}^{N_{\mathrm{B}}} = \mathrm{vec}[\mu_{l,j,n}^{(r,t)}|\forall t = 1:N_{\mathrm{B}}], \tag{19}$$

$$\mu_{l,j,n}^{(r,t)} = \mathrm{a}_{\mathrm{U},n}^{(r)}(\theta_{\mathrm{U},l,j})e^{-\mathrm{j}2\pi\frac{n}{N_{\mathrm{C}}^{\prime}T_s}\tau_{l,j}}(\mathrm{a}_{\mathrm{B},n}^{(t)}(\theta_{\mathrm{B},l,j}))^*, \tag{20}$$

where $\mathrm{a}_{\mathrm{U},n}^{(r)}(\theta_{\mathrm{U},l,j})$ and $\mathrm{a}_{\mathrm{B},n}^{(t)}(\theta_{\mathrm{B},l,j})$ denote the rth and the tth elements of $\mathbf{a}_{\mathrm{U},n}(\theta_{\mathrm{U},l,j})$ and $\mathbf{a}_{\mathrm{B},n}(\theta_{\mathrm{B},l,j})$ in (4) and (2), respectively. It should be noted that $\mathrm{a}_{\mathrm{U},n}^{(r)}(\theta_{\mathrm{U},l,j})$ and $\mathrm{a}_{\mathrm{B},n}^{(t)}(\theta_{\mathrm{B},l,j})$ are functions of $\mathbf{x}$, ϑ and $\mathbf{v}_{l,j}$ via (6)–(11).

III. The Proposed SLCE Algorithm

In this section, we formulate the UE localization problem, and then point out its challenges. After that, we will elaborate the proposed SLCE algorithm.

A. Problem Formulation

The mmWave MIMO-based SLCE can be formulated as the following optimization problem:

$$\mathscr{A}_{\mathrm{SLCE}} : (\hat{\boldsymbol{\beta}}, \hat{\mathbf{h}}) = \arg\min_{\boldsymbol{\alpha},\mathbf{h}} \mathbb{E}\{\|\mathbf{z} - \mathbf{g}(\boldsymbol{\beta}, \mathbf{h})\|_2^2. \tag{21}$$

where $\mathbb{E}\{\bullet\}$ stands for the expectation over $\boldsymbol{\epsilon}$.

Challenge: The above SLCE problem is non-convex with respect to (w.r.t.) $(\boldsymbol{\beta}, \mathbf{h})$, due to the nonlinear function $\mathbf{g}(\boldsymbol{\beta}, \mathbf{h})$. Moreover, in addition to the UE location parameters $\{\mathbf{x}, \vartheta\}$, there are too many nondeterministic parameters, e.g., $\mathbf{v}$ and $\mathbf{h}$, in the above SLCE problem, which complicates the estimate of UE location parameters. □

For the first challenge, we propose an efficient successive convex approximation (SCA)-based SLCE algorithm to overcome the non-convex optimization, which will be elaborated shortly. To address the second challenge, we adopt a channel package-up method, where all unknown propagation parameters of each NLOS path are absorbed into one variable for joint estimate. As such, the number of parameters is reduced, leading to a low-cost SLCE solution different from [15].

Let $\mathrm{c}_{l,j,n}^{(r,t)} = \mathrm{a}_{\mathrm{U},n}^{(r)}(\theta_{\mathrm{U},l,j})h_{l,j}[k]\mu_{l,j,n}^{(r,t)}\mathrm{a}_{\mathrm{B},n}^{(t)*}(\theta_{\mathrm{B},l,j})$ denote the overall NLOS channel state associated with the (r,t)th receiver-transmitter antenna pair of the jth BS at the nth subcarrier, for the lth NLOS path. For convenience, we use the following notations,

$$\mathbf{c}_{j,n}^{(r,t)} \in \mathbb{C}^L = \mathsf{vec}[\mathrm{c}_{l,j,n}^{(r,t)}|\forall l = 1:L], \tag{22}$$

$$\mathbf{h}_{\mathsf{NLOS}}^{\mathsf{EQ}} = \mathsf{vec}[\mathbf{c}_{j,n}^{(r,t)}|\forall t, \forall r, \forall n, \forall m, \forall j], \tag{23}$$

where $\mathbf{h}_{\mathsf{NLOS}}^{\mathsf{EQ}}[k] \in \mathbb{C}^{LJMN_{\mathrm{U}}N_{\mathrm{C}}N_{\mathrm{B}}}$ denotes the NLOS channel vector. Let $\mathbf{h}_{\mathsf{EQ}} \in \mathbb{C}^{J+LJMN_{\mathrm{U}}N_{\mathrm{C}}N_{\mathrm{B}}} = [\mathbf{h}_{\mathsf{LOS}}; \mathbf{h}_{\mathsf{NLOS}}^{\mathsf{EQ}}]$ be the equivalent channel. Let $\boldsymbol{\chi} \in \mathbb{C}^{3+J+LJMN_{\mathrm{U}}N_{\mathrm{C}}N_{\mathrm{B}}} = [\boldsymbol{\alpha}; \mathbf{h}_{\mathsf{EQ}}]$ be the overall variable.

In such a case, the SLCE problem is reformulated as

$$\mathscr{A}_{\mathrm{SLCE}}^{\sharp} : \hat{\boldsymbol{\chi}} = \arg\min_{\boldsymbol{\chi}} \|\mathbf{z} - \mathbf{g}_{\mathsf{EQ}}(\boldsymbol{\chi})\|_2^2. \tag{24}$$

where the measurement function $\mathbf{g}_{\mathsf{EQ}}(\boldsymbol{\chi})$ is reformulated as

$$\mathbf{g}_{\mathsf{EQ}}(\boldsymbol{\chi}) = \underbrace{\mathbf{g}_{\mathsf{LOS}}(\boldsymbol{\alpha}, \mathbf{h}_{\mathsf{LOS}})}_{\text{LOS path}} + \underbrace{\mathbf{W}^{\mathsf{H}}\mathbf{h}_{\mathsf{NLOS}}^{\mathsf{EQ}}}_{\text{NLOS path}}, \tag{25}$$

where $\mathbf{g}_{\mathsf{LOS}}(\boldsymbol{\alpha}, \mathbf{h}_{\mathsf{LOS}}) \in \mathbb{C}^{N_{\mathrm{U}}N_{\mathrm{C}}MJ}$ is the LOS component of measurement model, given by

$$\mathbf{g}_{\mathsf{LOS}}(\boldsymbol{\alpha}, \mathbf{h}_{\mathsf{LOS}}) = \mathbf{G}_{\mathsf{LOS}}(\boldsymbol{\alpha})\mathbf{h}_{\mathsf{LOS}}, \tag{26}$$

and $\mathbf{G}_{\mathsf{LOS}}(\boldsymbol{\alpha}) \in \mathbb{C}^{N_{\mathrm{U}}N_{\mathrm{C}}MJ \times J}$ is the coefficient matrix of LOS channel coefficient vector $\mathbf{h}_{\mathsf{LOS}}$, given by

$$\mathbf{G}_{\mathsf{LOS}}(\boldsymbol{\alpha}) = \mathrm{diag}\{\boldsymbol{g}_{0,j}|\forall j = 1:J\}, \tag{27}$$

$$\boldsymbol{g}_{0,j} \in \mathbb{C}^{N_{\mathrm{U}}N_{\mathrm{C}}M} = \mathrm{vec}[(\mathrm{g}_{0,j}^{(r)}[n,m])^*|\forall r, \forall n, \forall m], \tag{28}$$

where $\mathrm{g}_{0,j}^{(r)}[n,m]$ is given by (18) for $l = 0$. In addition, $\mathbf{W} \in \mathbb{C}^{LJMN_{\mathrm{U}}N_{\mathrm{C}}N_{\mathrm{B}} \times JMN_{\mathrm{U}}N_{\mathrm{C}}}$ denotes the known pilot symbol matrix, given by

$$\mathbf{W} = \mathsf{diag}[\mathbf{W}_j[n,m]|\forall n, \forall m, \forall j], \tag{29}$$

$$\mathbf{W}_j[n,m] \in \mathbb{C}^{N_{\mathrm{U}}N_{\mathrm{B}}L \times N_{\mathrm{U}}} = \mathbf{I}_{N_{\mathrm{U}}} \otimes \mathbf{w}_j[n,m], \tag{30}$$

$$\mathbf{w}_j[n,m] \in \mathbb{C}^{N_{\mathrm{B}}L} = \mathbf{1}_L \otimes \boldsymbol{\omega}_j[n,m], \tag{31}$$

in which $\mathbf{1}_L$ is an L-dimensional all-one vector.

B. Algorithm Development

For the non-convex optimization, there are already methods to identify the globally optimal solution, e.g., branch-and-bound algorithm [17]. However, such global search algorithm usually has a high computational complexity. In addition, conventional optimization methods, such as [18] and [19], usually depend on gradient descent, which will lead to a slow convergence rate when the solution is close to the optimum. Hence, it is non-trivial to develop an efficient algorithm handling the non-convex optimization challenge.

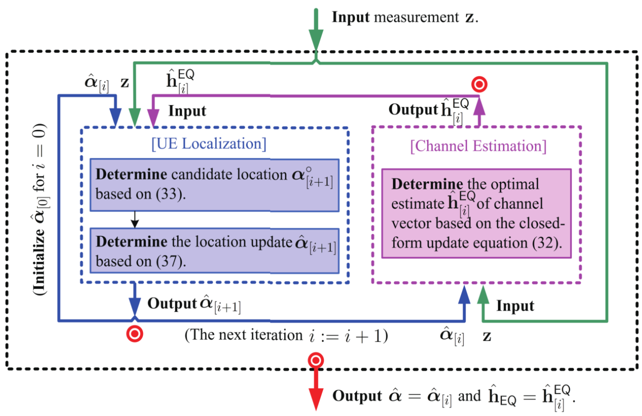

Fig. 2. Illustration of the main SLCE diagram.

Although $\mathscr{A}^{\sharp}_{\text{SLCE}}$ is non-convex w.r.t. $\boldsymbol{\chi}$, there is a hidden convex sub-structure w.r.t. $\mathbf{h}_{\mathsf{EQ}}$, given $\hat{\boldsymbol{\alpha}}$, since the measurement function $\mathbf{g}_{\mathsf{EQ}}(\boldsymbol{\chi})$ is linear w.r.t. $\mathbf{h}_{\mathsf{EQ}}$ as shown in (25). By using such hidden convex structure, we decompose the SLCE problem $\mathscr{A}^{\sharp}_{\text{SLCE}}$ into two components, i.e., the (convex) channel estimate and the (non-convex) UE localization. In other words, we shall successively perform the alternating optimization of $\boldsymbol{\alpha}$ and $\mathbf{h}_{\mathsf{EQ}}$, to achieve a joint localization and channel estimate for mmWave MIMO systems.

Specifically, starting from an initial point $\hat{\boldsymbol{\alpha}}_{[0]}$, the proposed SLCE algorithm will alternatively update $\hat{\boldsymbol{\alpha}}_{[i]}$ and $\hat{\mathbf{h}}^{\mathsf{EQ}}_{[i]}$ (corresponding to localization and channel estimate, respectively). The iteration will be repeated till $\hat{\boldsymbol{\alpha}}_{[i]}$ and $\hat{\mathbf{h}}^{\mathsf{EQ}}_{[i]}$ converge. The main diagram of SLCE is illustrated in Fig. 2.

1) Channel Estimate: For the convex variable $\mathbf{h}_{\mathsf{EQ}}$, given a fresh estimate $\hat{\boldsymbol{\alpha}}_{[i]}$ of $\boldsymbol{\alpha}$ (which will be elaborated by (33)), we directly derive its least square solution as per $\mathscr{A}^{\sharp}_{\text{SLCE}}$ in (24), which is the optimal estimation conditioned on $\hat{\boldsymbol{\alpha}}_{[i]}$ due to the linear Gaussian model (25). Namely, $\hat{\mathbf{h}}^{\mathsf{EQ}}_{[i]}$ is given by

$$\hat{\mathbf{h}}^{\mathsf{EQ}}_{[i]} = \left(\boldsymbol{\mathcal{W}}(\hat{\boldsymbol{\alpha}}_{[i]})\boldsymbol{\mathcal{W}}^{\mathrm{H}}(\hat{\boldsymbol{\alpha}}_{[i]})\right)^{-1}\boldsymbol{\mathcal{W}}(\hat{\boldsymbol{\alpha}}_{[i]})\,\mathbf{z}, \tag{32}$$

where $\boldsymbol{\mathcal{W}}(\hat{\boldsymbol{\alpha}}_{[i]}) \in \mathbb{C}^{(LJMN_{\mathrm{U}}N_{\mathrm{C}}N_{\mathrm{B}}+J)\times JMN_{\mathrm{U}}N_{\mathrm{C}}}$ dependent on $\hat{\boldsymbol{\alpha}}_{[i]}$ is given by is given by $\boldsymbol{\mathcal{W}} = [\mathbf{G}^{\mathrm{H}}_{\mathsf{LOS}}, \mathbf{W}]$. The fresh estimate $\hat{\boldsymbol{\alpha}}_{[i]}$ at the ith iteration is determined as follows.

2) UE Localization: For the non-convex problem associated with $\boldsymbol{\alpha}$, we propose an efficient SCA method by exploiting a convex approximation to the cost function in (24). Specifically, we iteratively solve the following convex subproblem $\mathscr{A}^{\sharp}_{\text{SLCE},[i]}$ to find a candidate update $\boldsymbol{\alpha}^{\circ}_{[i+1]}$,

$$\mathscr{A}_{\text{SLCE},[i]} : \boldsymbol{\alpha}^{\circ}_{[i+1]} = \arg\min_{\boldsymbol{\alpha}} f_{\mathrm{S}}\big(\boldsymbol{\alpha}; \hat{\boldsymbol{\alpha}}_{[i]}, \hat{\mathbf{h}}^{\mathsf{EQ}}_{[i]}\big), \tag{33}$$

where $f_{\mathrm{S}}\big(\boldsymbol{\alpha}; \hat{\boldsymbol{\alpha}}_{[i]}, \hat{\mathbf{h}}^{\mathsf{EQ}}_{[i]}\big)$ stands for the convex surrogate function of the original cost function in (24), given by (34), where $\nabla_{\boldsymbol{\alpha}}\mathbf{g}_{\mathsf{EQ}}\big(\hat{\boldsymbol{\alpha}}_{[i]}; \hat{\mathbf{h}}^{\mathsf{EQ}}_{[i]}\big) \in \mathbb{C}^{3\times JMN_{\mathrm{U}}N_{\mathrm{C}}}$ is given by (39) in Appendix A.

It should be noted that $f_{\mathrm{S}}\big(\boldsymbol{\alpha}; \hat{\boldsymbol{\alpha}}_{[i]}, \hat{\mathbf{h}}^{\mathsf{EQ}}_{[i]}\big)$ is different from the standard gradient-based surrogate function $f_{\mathrm{G}}\big(\boldsymbol{\alpha}; \hat{\boldsymbol{\alpha}}_{[i]}, \hat{\mathbf{h}}^{\mathsf{EQ}}_{[i]}\big)$ given by (35) that is usually adopted in conventional methods, e.g., [18] and [19]. In addition, $f_{\mathrm{S}}\big(\boldsymbol{\alpha}; \hat{\boldsymbol{\alpha}}_{[i]}, \hat{\mathbf{h}}^{\mathsf{EQ}}_{[i]}\big)$ preserves the second-order structure of the original cost function in (24). In consequence, our SCA-based SLCE algorithm will lead to a faster convergence speed than conventional gradient-based methods, which will be verified by simulations.

At each iteration, the subproblem $\mathscr{A}^{\sharp}_{\text{SLCE},[i]}$ is strictly convex, and the closed-form expression of $\boldsymbol{\alpha}^{\circ}_{[i+1]}$ is given by

$$\boldsymbol{\alpha}^{\circ}_{[i+1]} = \hat{\boldsymbol{\alpha}}_{[i]} + \underbrace{\left(\nabla^{\mathrm{H}}_{\boldsymbol{\alpha}}\mathbf{g}_{\mathsf{EQ}}\big(\hat{\boldsymbol{\alpha}}_{[i]}; \hat{\mathbf{h}}^{\mathsf{EQ}}_{[i]}\big)\right)^{\dagger}\left(\mathbf{z} - \mathbf{g}_{\mathsf{EQ}}\big(\hat{\boldsymbol{\alpha}}_{[i]}; \hat{\mathbf{h}}^{\mathsf{EQ}}_{[i]}\big)\right)}_{\mathbf{p}_{[i]}}, \tag{36}$$

where † denotes the pseudo-inverse, and $\mathbf{p}_{[i]}$ denotes its update direction that is different from the gradient. Given $\mathbf{p}_{[i]}$, the new update $\hat{\boldsymbol{\alpha}}_{[i+1]}$ is given by

$$\hat{\boldsymbol{\alpha}}_{[i+1]} = \hat{\boldsymbol{\alpha}}_{[i]} + \gamma_{[i]}\mathbf{p}_{[i]}, \tag{37}$$

where $\gamma_{[i]}$ is the step size subject to Armijo rule (38), in which $f\big(\boldsymbol{\alpha}; \hat{\mathbf{h}}^{\mathsf{EQ}}_{[i]}\big) = \big\|\mathbf{z} - \mathbf{g}_{\mathsf{EQ}}\big(\boldsymbol{\alpha}; \hat{\mathbf{h}}^{\mathsf{EQ}}_{[i]}\big)\big\|^2_2$ is the cost function of the original problem $\mathscr{A}^{\sharp}_{\text{SLCE}}$ given $\hat{\mathbf{h}}^{\mathsf{EQ}}_{[i]}$, and $\nabla_{\boldsymbol{\alpha}} f\big(\hat{\boldsymbol{\alpha}}_{[i]}; \hat{\mathbf{h}}^{\mathsf{EQ}}_{[i]}\big) = \nabla^{\mathrm{H}}_{\boldsymbol{\alpha}}\mathbf{g}_{\mathsf{EQ}}\big(\hat{\boldsymbol{\alpha}}_{[i]}; \hat{\mathbf{h}}^{\mathsf{EQ}}_{[i]}\big)\big(\mathbf{g}_{\mathsf{EQ}}\big(\hat{\boldsymbol{\alpha}}_{[i]}; \hat{\mathbf{h}}^{\mathsf{EQ}}_{[i]}\big) - \mathbf{z}\big) \in \mathbb{R}^{2JL+3}$ denotes the gradient vector of $f\big(\boldsymbol{\alpha}; \hat{\mathbf{h}}^{\mathsf{EQ}}_{[i]}\big)$ w.r.t. $\boldsymbol{\alpha}$ around $\boldsymbol{\alpha} = \hat{\boldsymbol{\alpha}}_{[i]}$. A legal $\gamma_{[i]}$ can be obtained by staring from a certain $\gamma_{[i]} > 0$ and repeatedly trying $\gamma_{[i]} = \nu\gamma_{[i]}$ with $\nu \in (0,1)$ till (38) is satisfied. Given a quadratic update vector $\mathbf{p}_{[i]}$, the Armijio rule (38) ensures a satisfied step length $\gamma_{[i]}$ at each iteration such that the cost function successively reduces till it converges. The obtained solution in (36) combining with (37) will finally result in a closed-form undate of $\hat{\boldsymbol{\alpha}}$.

C. Summary of Our SLCE Algorithm

Given an initial point $\hat{\boldsymbol{\alpha}}_{[0]}$, our SLCE algorithm alternatively optimizes $\boldsymbol{\alpha}$ and $\mathbf{h}_{\mathsf{EQ}}$ to find their best estimates. Once iterations converge, $\hat{\boldsymbol{\alpha}}$ and $\hat{\mathbf{h}}_{\mathsf{EQ}}$ will be determined. In addition, we use multiple samples to generate a good initial point $\hat{\boldsymbol{\alpha}}_{[0]}$. Namely, randomly generate multiple samples $\{\hat{\boldsymbol{\alpha}}^{(\kappa)}_{[0]}|\forall\kappa = 1 : K_S\}$ over parameter space, try all K_S samples, and then pick out the sample with minimum error as the initial point choice. The pseudo-code of the proposed SLCE approach is summarized in Algorithm 1.

Algorithm 1: The proposed SLCE algorithm

Input : The measurement sample $\mathbf{z}$.
Initialize $\hat{\boldsymbol{\alpha}}_{[0]}$.
While not converge **do** (for $i = 1 : M_{\mathrm{I}}$)
    Determine the channel state $\hat{\mathbf{h}}^{\mathsf{EQ}}_{[i]}$ as per (32).
    Find a candidate solution $\boldsymbol{\alpha}^{\circ}_{[i+1]}$ as per (36).
    Determine $\gamma_{[i]}$ as per (38).
    Determine $\hat{\boldsymbol{\alpha}}_{[i+1]}$ as per (37).
End
Determine the channel estimate $\hat{\mathbf{h}}_{\mathsf{EQ}} = \hat{\mathbf{h}}^{\mathsf{EQ}}_{[i]}$.
Determine the location estimate $\hat{\boldsymbol{\alpha}} = \hat{\boldsymbol{\alpha}}_{[i]}$.
Output: $\hat{\boldsymbol{\alpha}}$ and $\hat{\mathbf{h}}_{\mathsf{EQ}}$.

$$f_{\mathrm{S}}\big(\boldsymbol{\alpha};\hat{\boldsymbol{\alpha}}_{[i]},\hat{\mathbf{h}}^{\mathsf{EQ}}_{[i]}\big)=\big\|\mathbf{z}-\mathbf{g}_{\mathsf{EQ}}\big(\hat{\boldsymbol{\alpha}}_{[i]};\hat{\mathbf{h}}^{\mathsf{EQ}}_{[i]}\big)-\nabla^{\mathrm{H}}_{\boldsymbol{\alpha}}\mathbf{g}_{\mathsf{EQ}}\big(\hat{\boldsymbol{\alpha}}_{[i]};\hat{\mathbf{h}}^{\mathsf{EQ}}_{[i]}\big)\big(\boldsymbol{\alpha}-\hat{\boldsymbol{\alpha}}_{[i]}\big)\big\|_2^2. \tag{34}$$

$$f_{\mathrm{G}}\big(\boldsymbol{\alpha};\hat{\boldsymbol{\alpha}}_{[i]},\hat{\mathbf{h}}^{\mathsf{EQ}}_{[i]}\big)=\|\mathbf{z}-\mathbf{g}_{\mathsf{EQ}}\big(\hat{\boldsymbol{\alpha}}_{[i]};\hat{\mathbf{h}}^{\mathsf{EQ}}_{[i]}\big)\|_2^2+\|\boldsymbol{\alpha}-\hat{\boldsymbol{\alpha}}_{[i]}\|_2^2-2\big(\mathbf{z}-\mathbf{g}_{\mathsf{EQ}}\big(\hat{\boldsymbol{\alpha}}_{[i]};\hat{\mathbf{h}}^{\mathsf{EQ}}_{[i]}\big)\big)^{\mathrm{H}}\nabla^{\mathrm{H}}_{\boldsymbol{\alpha}}\mathbf{g}_{\mathsf{EQ}}\big(\hat{\boldsymbol{\alpha}}_{[i]};\hat{\mathbf{h}}^{\mathsf{EQ}}_{[i]}\big)\big(\boldsymbol{\alpha}-\hat{\boldsymbol{\alpha}}_{[i]}\big). \tag{35}$$

$$f(\hat{\boldsymbol{\alpha}}_{[i]}+\gamma_{[i]}\mathbf{p}_{[i]};\hat{\mathbf{h}}^{\mathsf{EQ}}_{[i]})\leq f(\hat{\boldsymbol{\alpha}}_{[i]};\hat{\mathbf{h}}^{\mathsf{EQ}}_{[i]})+a\gamma_{[i]}\nabla^{\mathrm{H}}_{\boldsymbol{\alpha}}f(\hat{\boldsymbol{\alpha}}_{[i]};\hat{\mathbf{h}}^{\mathsf{EQ}}_{[i]})\mathbf{p}_{[i]},\ \text{for } a>0. \tag{38}$$

IV. Numerical Results

In this section we shall provide numerical results to demonstrate the performance of the proposed SLCE algorithm.

A. Simulation Settings

We set the number of BS to be $J=3$ and the number of subcarriers to be $N'_{\mathrm{C}}=30$. We set $M=20$, $N_{\mathrm{B}}=N_{\mathrm{U}}=33$, carrier frequency $f_{\mathrm{C}}=60$GHz, sampling period $T_s=10$ns and light speed $c=3*10^8$m/s. Thus, λ_n and d_{A} can be determined via $\lambda_n=\frac{c}{\frac{n}{N'_{\mathrm{C}}T_s}+f_{\mathrm{C}}}$ and $d_{\mathrm{A}}=c/f_{\mathrm{C}}/2$, respectively. We assume a simple path loss model, i.e., $h_{l,j}=\frac{h'_{l,j}}{\wp^3_{l,j}}$, where $\wp_{l,j}$ is the path length, and $h'_{l,j}\sim\mathcal{N}_{\mathbb{C}}(0,1)$ is the small-scale fading. We set SNR = 20dB, unless specified otherwise, where $\mathrm{SNR}=\frac{\mathbb{E}\{\|\mathbf{g}_{\mathsf{EQ}}(\boldsymbol{\chi})\|_2^2\}}{\mathbb{E}\{\|\boldsymbol{\epsilon}\|_2^2\}}$, namely, the SNR is evaluated at the receiver side for fair comparison of different fading environments. Locations of UE and BSs are set at random within a squared area of $10^3\times10^3\mathrm{m}^2$, and their orientation angles are set at random. We set $L\in[1,5]$. We consider the following algorithms as baseline methods.

- **Baseline 1** [18]: It updates the unknown parameter as per the associated gradient vector.
- **Baseline 2** [19]: This algorithm employs the gradient with Armijo-type line search to update unknown parameters.
- **Baseline 3** [5]: This algorithm uses three-stage optimization integrating orthogonal matching pursuit, expectation maximization and Gauss-Seidel iteration methods.

Cramer-Rao lower bound (CRLB) on the error of UE location, orientation and small-scale fading coefficient is proposed in [15], which is used as the performance benchmark.

B. Simulation Results

The estimate errors of UE location, orientation and small-scale fading coefficient associated with various algorithms are presented in Fig. 3, 4 and 5, respectively. We can see that the proposed SLCE algorithm outperforms those baselines, in terms of both estimate error and convergence rate, due to our problem-specific update rule design in Section III-B. In addition, the proposed SLCE algorithm can almost reach the corresponding CRLB. It is shown that the proposed SLCE algorithm can achieve a localization error of 0.017[m] for $\mathrm{SNR}=20\,\mathrm{dB}$, under the given parameter settings.

In addition, the UE location estimate error and channel estimate error of the proposed SLCE algorithm v.s. SNR is given by Fig.6. It is shown that the SLCE error and its CRLB is linearly decreasing with the SNR.

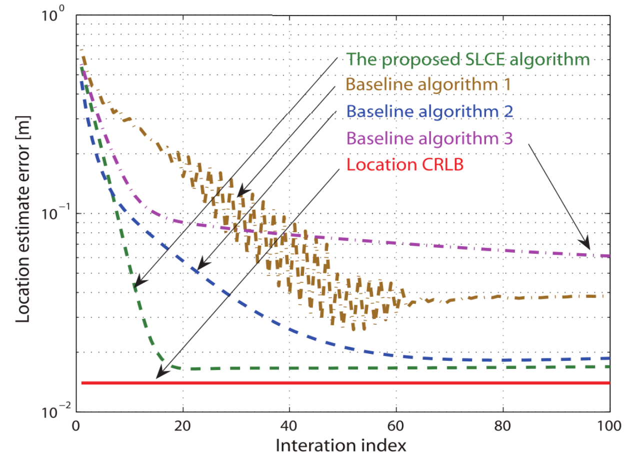

Fig. 3. UE location estimate error [m] of various algorithms.

V. Conclusions

In this paper, a novel SLCE algorithm is proposed to estimate UE location parameters over small-scale fading channel and multipath propagation environments for 5G mmWave MIMO systems. It is verified by simulations that the proposed SLCE method achieves a large performance gain over existing localization baselines, by harnessing the NLOS propagation. In addition, our SLCE algorithm renders a fast convergence rate due to the problem-specific update rule development.

Appendix A
Gradient Matrix

The gradient matrix in (34) is given by

$$\nabla_{\boldsymbol{\alpha}}\mathbf{g}_{\mathsf{EQ}}\big(\hat{\boldsymbol{\alpha}}_{[i]};\hat{\mathbf{h}}^{\mathsf{EQ}}_{[i]}\big)=\mathbf{D}_{\mathsf{LOS}}\boldsymbol{\mathcal{H}}_{\mathsf{LOS}}, \tag{39}$$

where $\mathbf{D}_{\mathsf{LOS}}\in\mathbb{C}^{3\times JMN_{\mathrm{C}}N_{\mathrm{U}}}$ is given by

$$\mathbf{D}_{\mathsf{LOS}}=[\mathbf{d}^{(r)}_{j,m,n}|\forall r,\forall n,\forall m,\forall j], \tag{40}$$

$$\mathbf{d}^{(r)}_{j,m,n}\in\mathbb{C}^3=\begin{bmatrix}\sum\limits_{t=1:N_{\mathrm{B}}}\omega_j^{(t)}[m,n]\mu^{(r,t)*}_{0,j,n}\,\boldsymbol{\varrho}^{(r,t)}_{0,j,n}\\ \sum\limits_{t=1:N_{\mathrm{B}}}\omega_j^{(t)}[m,n]\mu^{(r,t)*}_{0,j,n}\,\rho^{(r,t)}_{0,j,n}\end{bmatrix}, \tag{41}$$

wherein $\boldsymbol{\varrho}^{(r,t)}_{0,j,n}$ is given by (42) and $\rho^{(r,t)}_{0,j,n}$ is given by (43).

In addition, $\boldsymbol{\mathcal{H}}_{\mathsf{LOS}}\in\mathbb{C}^{JMN_{\mathrm{C}}N_{\mathrm{U}}\times JMN_{\mathrm{C}}N_{\mathrm{U}}}$ is given by

$$\boldsymbol{\mathcal{H}}_{\mathsf{LOS}}=\mathsf{diag}\{\boldsymbol{\mathcal{H}}^{\mathsf{LOS}}_j[k]|\forall j=1:J\}, \tag{44}$$

in which $\boldsymbol{\mathcal{H}}^{\mathsf{LOS}}_j\in\mathbb{C}^{MN_{\mathrm{C}}N_{\mathrm{U}}\times MN_{\mathrm{C}}N_{\mathrm{U}}}$ is given by

$$\boldsymbol{\mathcal{H}}^{\mathsf{LOS}}_j=\mathbf{I}_{MN_{\mathrm{C}}N_{\mathrm{U}}}\otimes(\hat{h}_{0,j,[i]})^*, \tag{45}$$

where * denotes the conjugate of complex numbers.

$$
\begin{aligned}
\boldsymbol{\varrho}_{l,j,n}^{(r,t)} =& \mathrm{j}2\pi\frac{n}{cN_{\mathrm{C}}^{\prime}T_s}\frac{\mathbf{x}-\mathbf{u}_j}{\|\mathbf{x}-\mathbf{u}_j\|_2} - \mathrm{j}\frac{d_{\mathrm{B}}\pi}{\lambda_n}(t-1)\frac{\|\mathbf{x}-\mathbf{u}_j\|_2^2\mathbf{e}_Y - (\mathbf{x}-\mathbf{u}_j)(\mathbf{x}-\mathbf{u}_j)^{\mathrm{H}}\mathbf{e}_Y}{\|\mathbf{x}-\mathbf{u}_j\|_2^3} \\
&+\mathrm{j}\frac{d_{\mathrm{U}}\pi}{\lambda_n}(r-1)\frac{\cos\left(\arccos\left(\frac{(\mathbf{x}-\mathbf{u}_j)^{\top}\mathbf{e}_X}{\|\mathbf{x}-\mathbf{u}_j\|_2}\right)-\vartheta\right)}{\sqrt{1-\left(\frac{(\mathbf{x}-\mathbf{u}_j)^{\top}\mathbf{e}_X}{\|\mathbf{x}-\mathbf{u}_j\|_2}\right)^2}}\frac{\|\mathbf{x}-\mathbf{u}_j\|_2^2\mathbf{e}_X - (\mathbf{x}-\mathbf{u}_j)(\mathbf{x}-\mathbf{u}_j)^{\mathrm{H}}\mathbf{e}_X}{\|\mathbf{x}-\mathbf{u}_j\|_2^3}.
\end{aligned}
\tag{42}
$$

$$
\rho_{l,j,n}^{(r,t)} = \mathrm{j}\frac{d_{\mathrm{U}}\pi}{\lambda_n}(r-1)\cos\left(\arccos\left(\frac{(\mathbf{x}-\mathbf{u}_j)^{\top}\mathbf{e}_X}{\|\mathbf{x}-\mathbf{u}_j\|_2}\right)-\vartheta\right)\right). \tag{43}
$$

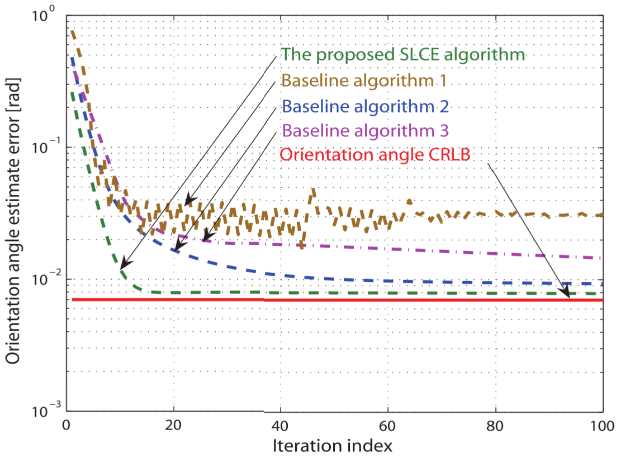

Fig. 4. UE orientation estimate error [rad] of various algorithms.

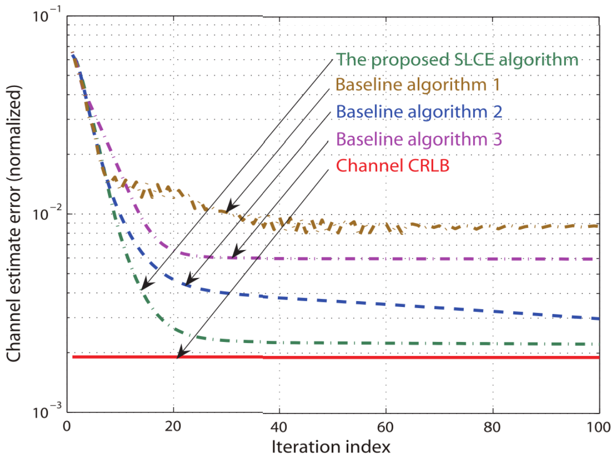

Fig. 5. Small-scale fading channel estimate errors (normalized).

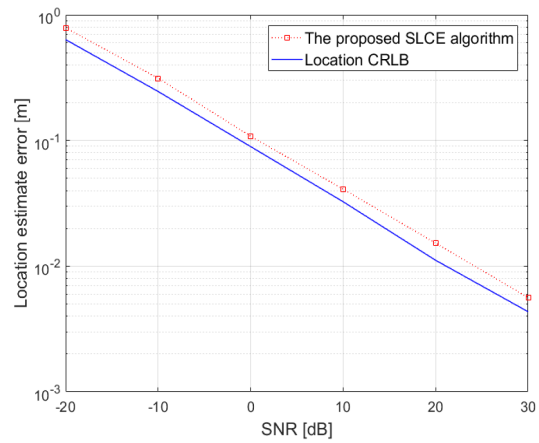

Fig. 6. The localization error of the proposed SLCE algorithm v.s. SNR.

REFERENCES

[1] Z. Pi and F. Khan, "An introduction to millimeter-wave mobile broadband systems," *IEEE Comm. Mag.*, vol. 49, no. 6, pp. 101-107, 2011.

[2] T. Rappaport, S. Sun, R. Mayzus, H. Zhao, Y. Azar, K. Wang, G. Wong, J. Schulz, M. Samimi, and F. Gutierrez, "Millimeter wave mobile communications for 5G cellular: It will work!" *IEEE Access*, vol. 1, pp. 335C349, 2013

[3] Z. Gao, L. Dai, D. Mi, Z. Wang, M. A. Imran, and M. Z. Shakir, "MmWave massive-MIMO-based wireless backhaul for the 5G ultra-dense network." *IEEE Wireless Communications* 22.5 (2015): 13-21.

[4] J. Brady, N. Behdad, and A. M. Sayeed, "Beamspace MIMO for millimeter-wave communications: System architecture, modeling, analysis, and measurements." *IEEE Transactions on Antennas and Propagation*, 61.7 (2013): 3814-3827.

[5] A. Shahmansoori, G. E. Garcia, G. Destino, G. Seco-Granados, and H. Wymeersch, "Position and Orientation Estimation through Millimeter Wave MIMO in 5G Systems," 2017.

[6] R. D. Taranto, S. Muppirisetty, R. Raulefs, D. Slock, T. Svensson, and H. Wymeersch, "Location-aware communications for 5G networks: How location information can improve scalability, latency, and robustness of 5G." *IEEE Signal Processing Magazine* 31.6 (2014): 102-112.

[7] K. Witrisal, P. Meissner, E. Leitinger, Y. Shen, C. Gustafson, F. Tufvesson, K. Haneda, D. Dardari, A. F. Molisch, A. Conti, M. Z. Win, "High-accuracy localization for assisted living: 5G systems will turn multipath channels from foe to friend." *IEEE Signal Processing Magazine* 33.2 (2016): 59-70.

[8] J. A. del Peral-Rosado, J. A Lopez-Salcedo, S. Kim, and G. Seco-Granados, "Feasibility study of 5G-based localization for assisted driving." *Localization and GNSS (ICL-GNSS), 2016 International Conference on*. IEEE, 2016.

[9] J. Clausen. "Branch and bound algorithms-principles and examples." *Department of Computer Science, University of Copenhagen*, 1999.

[10] S. Gezici, Z. Tian, G. B. Giannakis, H. Kobayashi, A. F. Molisch, H. V. Poor, and Z. Sahinoglu, "Localization via ultra-wideband radios: a look at positioning aspects for future sensor networks." *IEEE signal processing magazine* 22.4 (2005): 70-84.

[11] B. Zhou, Q. Chen, H. Wymeersch, P. Xiao and L. Zhao, "Variational Inference-based Positioning with Nondeterministic Measurement Accuracies and Reference Location Errors", *IEEE Transactions on Mobile Computing*, Vol.16, No.10, 2017, pp.2955-2969

[12] B. Zhou and Q. Chen, "On the Particle-assisted Stochastic Search Mechanism in Wireless Cooperative Localization", *IEEE Transactions on Wireless Communications,* Vol.15, No.7, pp.4765-4777, July, 2016

[13] B. Zhou, Q. Chen and P. Xiao, "Error Propagation Analysis of the Received Signal Strength-based Simultaneous Localization and Tracking in Wireless Sensor Networks", *IEEE Transactions on Information Theory*, Vol.63, No.6, 2017, pp.3983-4007

[14] B. Zhou, Q. Chen, P. Xiao and L. Zhao, "On the Spatial Propagation Characteristics of Cooperative Localization Errors in Wireless Network-

s", *IEEE Transactions on Vehicular Technology*, Vol.66, No,2, 2017, pp.1647-1658

[15] B. Zhou, A. Liu, and V. Lau, "Successive Localization and Beamforming in 5G mmWave MIMO Communication Systems", *IEEE Transactions on Signal Processing*, vol.67, no.6, 2019, pp.1620-1635

[16] D. Lee, H. Seo, B. Clerckx, E. Hardouin, D. Mazzarese, S. Nagata, and K. Sayana, "Coordinated multipoint transmission and reception in LTE-advanced: deployment scenarios and operational challenges." *IEEE Communications Magazine*, 50.2 (2012).

[17] E. L. Lawler, and D. E. Wood. "Branch-and-bound methods: A survey." *Operations research* 14.4 (1966): 699-719.

[18] A. Beck, and M. Teboulle. "Gradient-based algorithms with applications to signal recovery." *Convex optimization in signal processing and communications* (2009): 42-88.

[19] Y.-H. Dai, "Conjugate gradient methods with Armijo-type line searches." *Acta Mathematicae Applicatae Sinica*, 18.1 (2002): 123-130.